
PROVENANCE OF OLIGOCENE CONGLOMERATES AND ASSOCIATED SANDSTONES FROM THE SIAMANÁ FORMATION, SERRANÍA DE JARARA, GUAJIRA, COLOMBIA: IMPLICATIONS FOR OLIGOCENE CARIBBEAN-SOUTH AMERICAN TECTONICS

PROVENIENCIA DE ARENISCAS Y CONGLOMERADOS OLIGOCENOS PERTENECIENTES A LA FORMACIÓN SIAMANÁ, SERRANÍA DE JARARA, GUAJIRA, COLOMBIA: IMPLICACIONES EN LA TECTÓNICA OLIGOCENA DEL CARIBE Y SUR AMÉRICA

Sebastian Zapata^{1}; Marion Weber¹; Agustín Cardona^{2,3}; Víctor Valencia⁴; Georgina Guzmán⁵; Monica Tobón¹*

1. Universidad Nacional, Medellín, Colombia,

2. Smithsonian Tropical Research Institute, Panamá,

3. Corporación Geológica ARES,

4. Department of Geosciences, University of Arizona, 5INVEMAR, Santa Marta, Colombia.

5. INVEMAR, Santa Marta, Colombia

szapatah@gmail.com, mweber@unal.edu.co

Recibido para evaluación: 9 de Noviembre de 2009 / Aceptación: 7 de Mayo de 2010 / Recibida versión final: 28 de Junio de 2010

ABSTRACT

Analyses of composition and sedimentological attributes of conglomerate clasts together with petrographical and heavy mineral analyses and detrital geochronology from sandstones of the Oligocene Siamaná Formation in the Serranía de Jarara, are presented in order to reconstruct the provenance of this sedimentary sequence and contribute to the knowledge of the tectonosedimentary evolution of the Guajira Peninsula and the Caribbean.

The results indicate that the source areas are proximal and are located to the southeast. The presence of plutonic igneous and medium- to low-grade metamorphic rocks, as well as high-pressure metamorphic rocks, indicate that the lithostratigraphic units (Parashi Stock and Jarara Formation) of the Serranía de Jarara and an unidentified unit to the southeast, are the main rock sources. The heavy minerals and the detrital zircon distribution with peaks at approximately 50 Ma, 207 Ma, 245 Ma, 463 Ma, 963 Ma and 1044 Ma, confirm that this is the source area. The extremely proximate sources and the rapid burying of the basin, which is evident due to the presence of marine sediments that overlie this sequence, indicate that this siliciclastic unit is related to the initial phases of a pull-apart basin. This basin was probably formed as a result of the movement of the Caribbean plate towards the east. The origin of the high-pressure clasts is unknown, and is possibly linked to a tectonic mélange. The U-Pb ages of approximately 50 Ma and the presence of fragments from the Parashi Stock, suggest exhumation during the Eocene and Upper Oligocene, possibly linked to the formation of the basin.

KEY WORDS:

Colombia, Guajira, Caribbean plate, Oligocene, pull-apart basin, provenance.

RESUMEN

Se presentan los resultados de análisis de composición y de atributos sedimentológicos de clastos de conglomerados, junto con la caracterización petrográfica, el análisis de minerales pesados y geocronología detrítica U-Pb en circones de areniscas de la Formación Siamaná de edad Oligoceno de la Serranía del Jarara, para reconstruir la procedencia y contribuir al conocimiento de la evolución tectonosedimentaria de la Península de la Guajira y el Caribe.

El conjunto de resultados indican que las áreas de aporte son de carácter proximal y están localizadas al sureste. La presencia de material derivado fundamentalmente de rocas ígneas plutónicas y metamórficas de medio a bajo grado así como fragmentos de rocas de alta presión indica que la Serranía de Jarara y sus unidades litoestratigráficas (Stock de Parashi y Formación Jarara), y un área no reconocida al sureste representan las áreas de aporte fundamental de esta secuencia. Los resultados de minerales pesados y las poblaciones de circones detriticos con picos de distribución de aproximadamente 50 Ma, 207 Ma, 245 Ma, 463 Ma, 963 Ma and 1044 Ma confirman esta área de aporte. Las fuentes extremadamente proximales de esta secuencia y el posterior hundimiento de la cuenca, evidenciado por los sedimentos marinos que los suprayacen, indican que esta secuencia siliciclastica está asociada a las fases iniciales de un ambiente de pull-apart, que formó esta cuenca por el avance hacia el este de la placa Caribe. El origen de los clastos de alta presión de fuente desconocida posiblemente están ligados a un mélange tectónico. Las edades U-Pb de aproximadamente 50 Ma y la presencia de clastos afines con el Stock de Parashi implican una importante fase de exhumación durante el Eoceno y Oligoceno Superior, que estaría en parte asociada a la formación de la cuenca.

PALABRAS CLAVES:

Colombia, Guajira, Placa Caribe, Oligoceno, cuencas pull-apart, procedencia.

1. INTRODUCTION

Following the Late Cretaceous to Paleogene arc-continent collision between the Caribbean front and the northwestern South American Continent in the southern margin of the Caribbean plate (Pindell et al., 2005; Weber et al., 2009), Eocene to Miocene basin formation and infill recorded in the Upper Guajira Peninsula of Colombia indicate a subsequent oblique to strike-slip convergence of the Caribbean plate and the South American plate (Pindell, 1993; Avé Lallement and Sisson, 1993; Macellari, 1995; Pindell et al., 1998; Montes et al., 2005; Ramirez, 2006; Gorney et al., 2007; Vence, 2008; Pindell and Keenan, 2009).

The Siamaná Formation of the Guajira Peninsula represents a major Oligocene unconformity, related to the formation of one of the major Oligocene to Neogene pull-apart basins built by the west to east migration of the Caribbean plate and the segmentation of the once coherent Andean blocks (Pindell 1993, Avé Lallement and Sisson, 1993; Macellari, 1995, Montes et al., 2005; 2009; Ramirez, 2006; Gorney et al., 2007; Vence, 2008).

In this contribution we reconstruct the provenance record from an Oligocene conglomerate and associated sandstone sequence of the Siamaná Formation, which lies on the northwestern foothills of the Serranía de Jarara, by means of clast counting, sandstone petrography, heavy mineral analysis and detrital zircon geochronology. Due to limited transport of this type of sedimentary material (Boggs, 2009), conglomerate provenance is used to constrain the uplift and exhumation history in the source area, and to test the regional tectonic model for pull-apart basin formation, which predicts that at the source of the basin sediments must be extremely proximal.

2. GEOLOGICAL SETTING

The Guajira Peninsula is located in northern Colombia, and is formed by small and isolated hilly massifs (Serranías), separated by Oligocene basins filled by Cretaceous and Cenozoic sediments (MacDonald, 1964; Lockwood, 1965; Alvarez, 1967; Vence, 2008) (Figure 1). The central massif is the Serranía de Jarara, which has a roughly southeast to northwestern trend.

The Serranía de Jarara can be divided into two main metamorphic belts: (1) a southeastern belt of amphibolites, mica schists and associated orthogneisses (Macuira Group), intruded by Jurassic granitoids (Lockwood, 1965; Cardona-Molina et al., 2006; Weber et al., 2009). Recent U-Pb geochronology on the orthogneisses have yielded Early Triassic ages of ca. 245 Ma, which may be linked to a late metamorphic event (Weber et al., 2010). (2) To the northwest, two major Cretaceous metamorphic units are exposed: (a) The Jarara Formation formed by graphitic phyllites, muscovite schists, chlorite schists and meta-volcanic rocks, biotite schists and gneisses, and calcite marbles (Lockwood, 1965). (b) The Etpana Formation, formed by phyllites, greenschists, large bodies of serpentinites, gabbros and rodingites (Lockwood, 1965; Arredondo, 2005) (Figure 1). These rocks are intruded by quartzdiorites and porphyritic rocks of the Eocene Parashi Stock (Lockwood, 1965; Cardona et al., 2007).

Farther to the west, Weber et al. (2009) have identified the existence of an accreted island arc remnant that collided with the continental margin in the Maastrichian. This collision is evident in the metamorphism of the Jarara and Etpana formations (Weber et al., 2010).

The sedimentary record of the Guajira Peninsula includes major Jurassic to Cretaceous rocks exposed in the southeast (MacDonald 1964; Rollins, 1965; Toussaint, 1996) (Figure 1), with stratigraphic features that can be correlated with the sedimentary record of the adjacent eastern Andes of Colombia (Toussaint, 1996; Villamil, 1999).

During the Eocene, the migration of the Caribbean plate towards the east was responsible for the formation of several pull-apart basins (Muessig, 1984; Macellari, 1995; Gorney et al., 2007). In the Guajira region this scenario was marked by the dextral displacements of the Cuisa and Oca faults, and the generation of pull-apart or graben-type basins in the Baja and Alta Guajira (Vence, 2008; Macellari, 1995) (Figure 1). This new period of sedimentation apparently included the deposition of a series of conglomerates, marls and calcareous shales of the Siamaná Formation on top of the older

Macarao Formation or directly on the crystalline rocks (Lockwood, 1965). Deep water sediments of the Uitpa Formation and Miocene shallow water Formations like Jimol and Castilletes were deposited on top of the Siamaná Formation confirming the deepening of the basin.

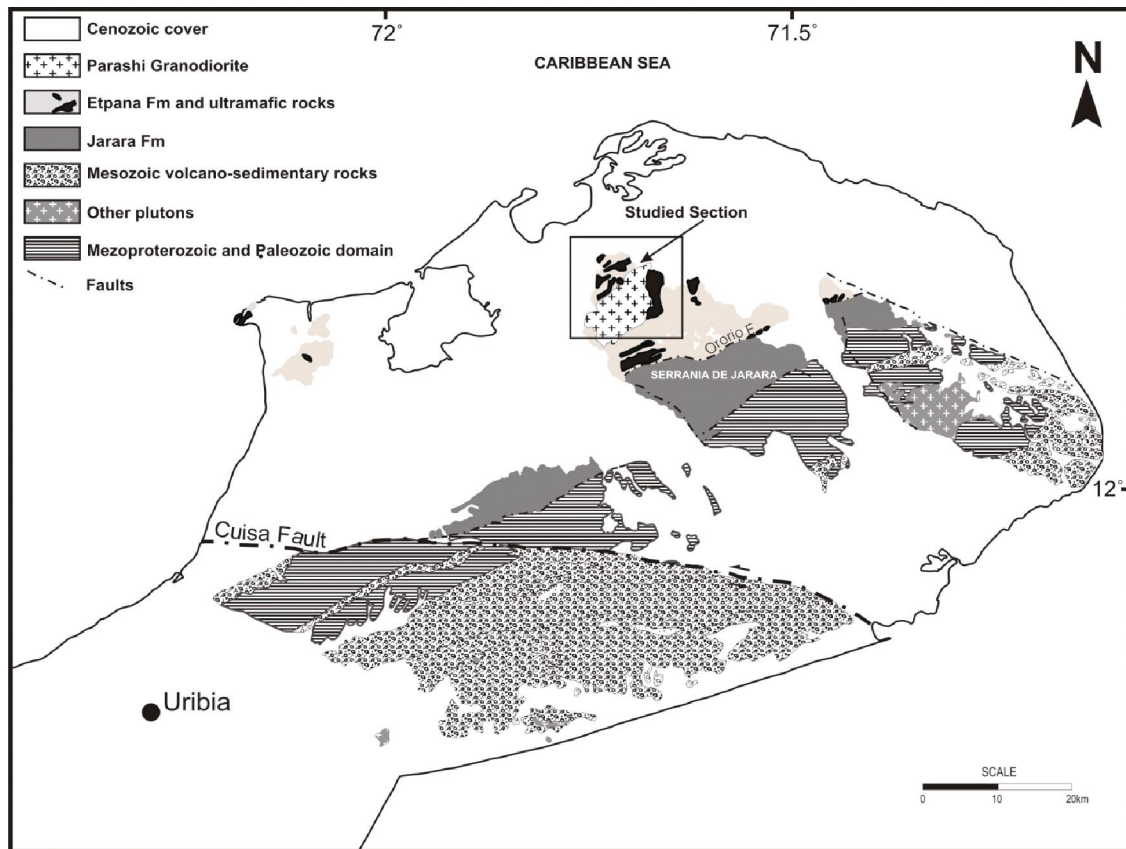


Figure 1. Geological settings and location of the studied section of the Siamaná Formation, modified from the Geological Map of Colombia (Ingeominas, 1997).

The conglomerate unit selected for provenance analysis is part of the Siamaná Formation in the Serranía de Jarara (Lockwood, 1965). This conglomerate contains a series of high-pressure Cretaceous metamorphic clasts whose origin is linked to the subduction and collision of the Caribbean arc front against the South American continent (Green et al., 1968; Zapata, 2005; Weber et al., 2007). Finding the in-situ origin of these high-pressure rocks has proven to be challenging (Lockwood et al., 1965; Green et al., 1968; Weber et al., 2007; 2009), however their regional petrotectonic evolution link them to the adjacent rocks of the Etpana Formation (Weber et al., 2007; 2010).

3. ANALYTICAL TECHNIQUES

Heavy minerals were extracted after crushing and washing, using LST liquid with a density of 2.89. Grains were mounted on a glass slide using meltmount® resin, that has an refraction index of 1.54.

Detrital zircons were extracted from sandstones following standard procedures for manual crushing and heavy liquid and magnetic separation at the University of Arizona, in Tucson. Once separated, the detrital zircons were encased in epoxy within one-inch ring mounts, which were then sanded and polished to produce a smooth flat surface that exposed the interiors of the zircon grains. Analytical procedures followed Gehrels et al. (2006, 2008). Zircon grains were selected randomly from all sizes and shapes, although grains with obvious cracks or inclusions were avoided. U/Pb ages of detrital zircons were obtained using an LA-MC-ICP-MS (GVI Isoprobe; GV Instruments, Manchester,

UK). The interiors of the zircon grains were ablated using a New Wave DUV193 Excimer laser (New Wave Instruments, Provo, UT, USA, and Lambda Physik Inc., Ft. Lauderdale, FL, USA) operating at a wavelength of 193 nm and using a spot diameter of 35–50 mm; laser ablation pits are ~20 mm deep. With the LA-MC-ICP-MS, the ablated material is carried via argon gas to the plasma source of a Micromass Isoprobe, which is configured in such a way that U and Pb can be measured simultaneously. Measurements were made in the static mode using Faraday collectors for ^{238}U , ^{232}Th , ^{208}Pb , ^{207}Pb , ^{206}Pb and an ion counting channel for ^{204}Pb . Analyses consist of one 20-s integration with the peak centered but no laser firing (checking background levels), and 20 1-s integrations with the laser firing on the zircon grain. At the end of each analysis, a 30-s delay occurs during which the previous sample is purged from the system and the peak signal intensity returns to background levels. The contribution of Hg to the ^{204}Pb is accounted for by subtracting the background values.

Common lead corrections were made using the measured ^{204}Pb of the sample and assuming initial Pb compositions from Stacey and Kramers (1975). A fragment of a zircon crystal of known age (564 ± 4 Ma, 2 s error; G. E. Gehrels, unpublished data) was analyzed after every fifth zircon analysis to correct for inter-element and Pb isotope fractionation. The ages presented are $^{206}\text{Pb}/^{238}\text{U}$ ages for grains with ages <1000 Ma and $^{207}\text{Pb}/^{206}\text{Pb}$ ages for grains with ages >1000 Ma. All uncertainties of individual grains were reported at the first level and include only measurement errors; systematic errors would have increased age uncertainties by 1–2%. Those analyses with or more than 20% discordance or 5% reverse discordance were omitted from further consideration. The data from each sample were displayed on concordia diagrams and age probability plots/ histograms using the programs of Ludwig (2003). Age probability plots

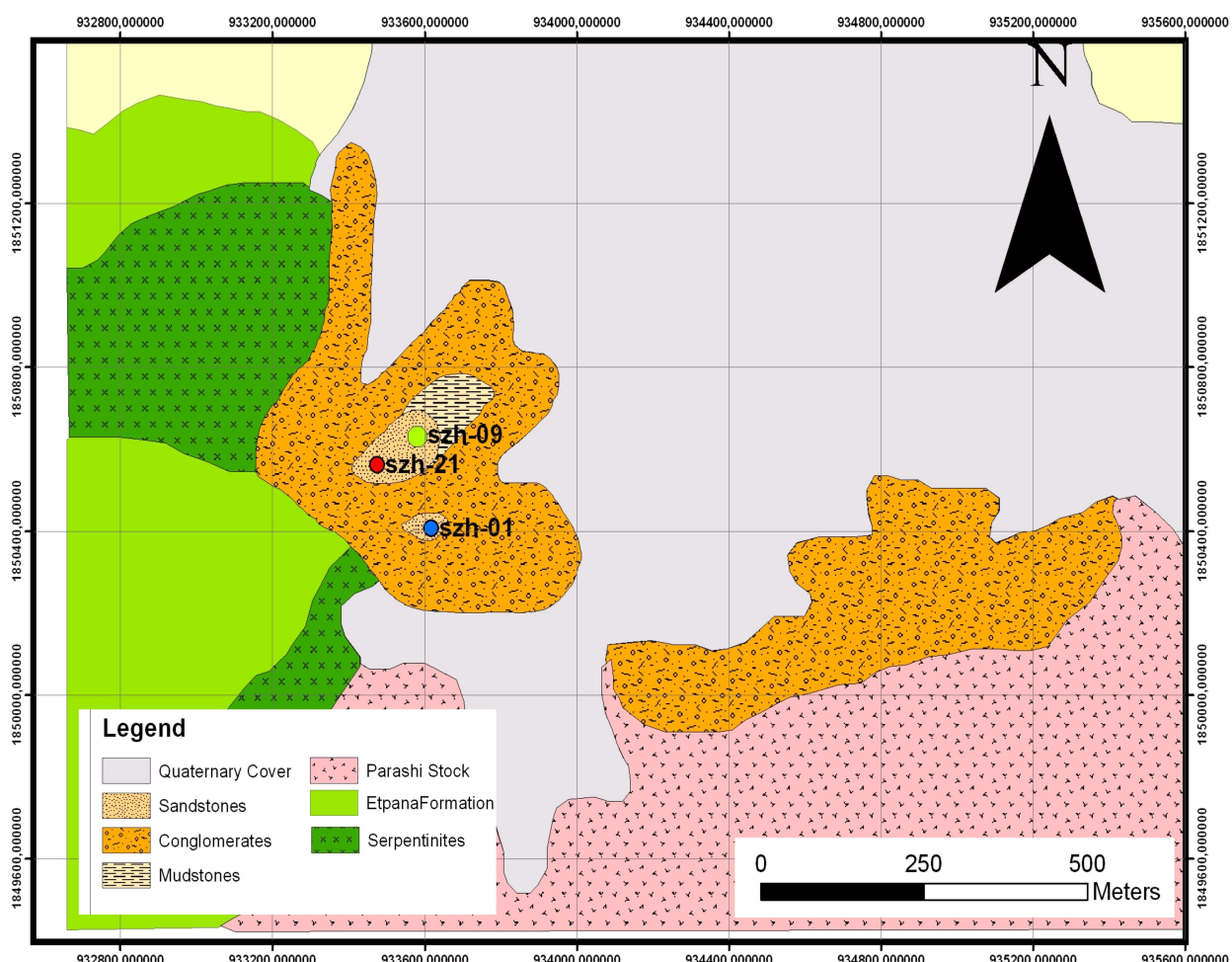


Figure 2. Studied section located in the NW of the Serranía de Jarara. Symbols represent collected sandstone samples.

depicted each age and its uncertainty as a normal distribution, summing all ages from the analyzed zircons of a sample into one curve, which was then divided by the total number of analyzed zircons.

4. RESULTS

The study section is located in the northwestern boundary of the Serranía de Jarara. The size of this section is approximately 1 Km² and 24 m thick (Figures 2 and 3). This conglomerate rests on top of ultramafic rocks and schists that are part to the Etpana Formation (Figure 2). Although not studied, another conglomerate exposed to the east, apparently rests directly on top of the Eocene Parashi Granitoid. It is possible to distinguish three units in the studied section of the Siamaná Formation (Figure 3). The lower unit comprises a 20 m thick conglomerate, which is overlain by a 3 m thick layer of calcareous sandstones. Also present is a 4 m mudstone lens associated to the sandstones and resting on top of the conglomerates (Figure 3).

5. CONGLOMERATE PROVENANCE ANALYSIS

Sediment sorting, composition, size, and roundness were quantified in 9 stations (C1 to C9, Figure 4) of a single conglomeratic layer. Distribution maps of sedimentological properties were drawn from the collected data.

Systematic observation of clastic elements has shown that materials tend to decrease in size towards the current direction (Pettijohn, 1975) and therefore, the average clast size distribution is an indicator of the possible location of the depocenter of the materials found in the conglomeratic unit. In general in the studied section the largest rocks are located to the southwest, decreasing in a radial pattern towards the northeast (Figure 4B).

Variation in sediment sorting is directly related to decrease of grain size and can be used to identify flow direction (Pettijohn, 1975). Sorting of the conglomerate in station C1 is very poor, with sizes ranging between 2 cm to 60 cm (Figure 4A). In station C3, located towards the center of the unit, sorting is defined by an unimodal grain distribution, whereas stations C6 and C9, which are located on the edges of the conglomerate, show good sorting, with sizes of ca. 35 cm and 25 cm respectively (Figure 4A). This trend clearly shows a general increase in sediment sorting towards the northeast.

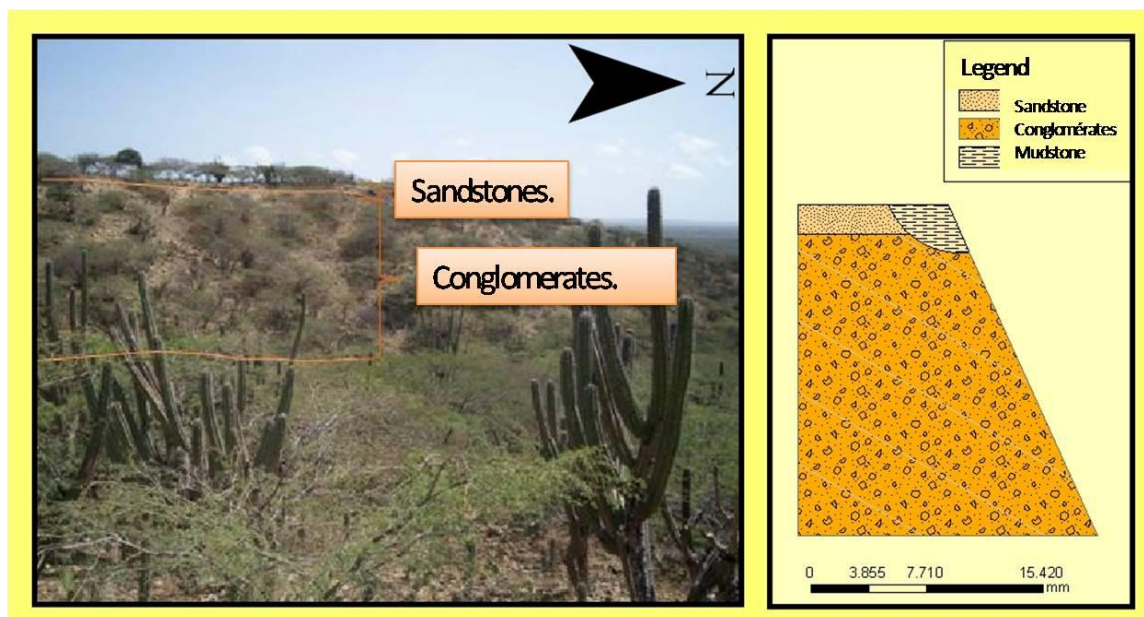


Figure 3. Studied stratigraphic section of the Siamaná Formation.

These features and the fact that the sorting pattern is inversely related to grain size (Figures 4A, 4B), confirms that the stream direction was to the northeast.

The composition of the clasts includes granodiorites and porphyritic rocks, quartzites, serpentized ultramafic rocks, high-pressure metapelites, eclogites and muscovite-quartz schists. Figure 4C shows the percentages of abundance of each composition in representative stations.

Roundness and sphericity are considered to increase with the amount of sediment transport (Pettijhon, 1975). In the case of the conglomerate of the studied section, roundness of the clasts increases towards the fringes, and is lowest to the center-southwest of the deposit (Figure 4D), indicating that the clasts to the southeast were exposed to longer travel distances and therefore were subjected longer to sediment transport.

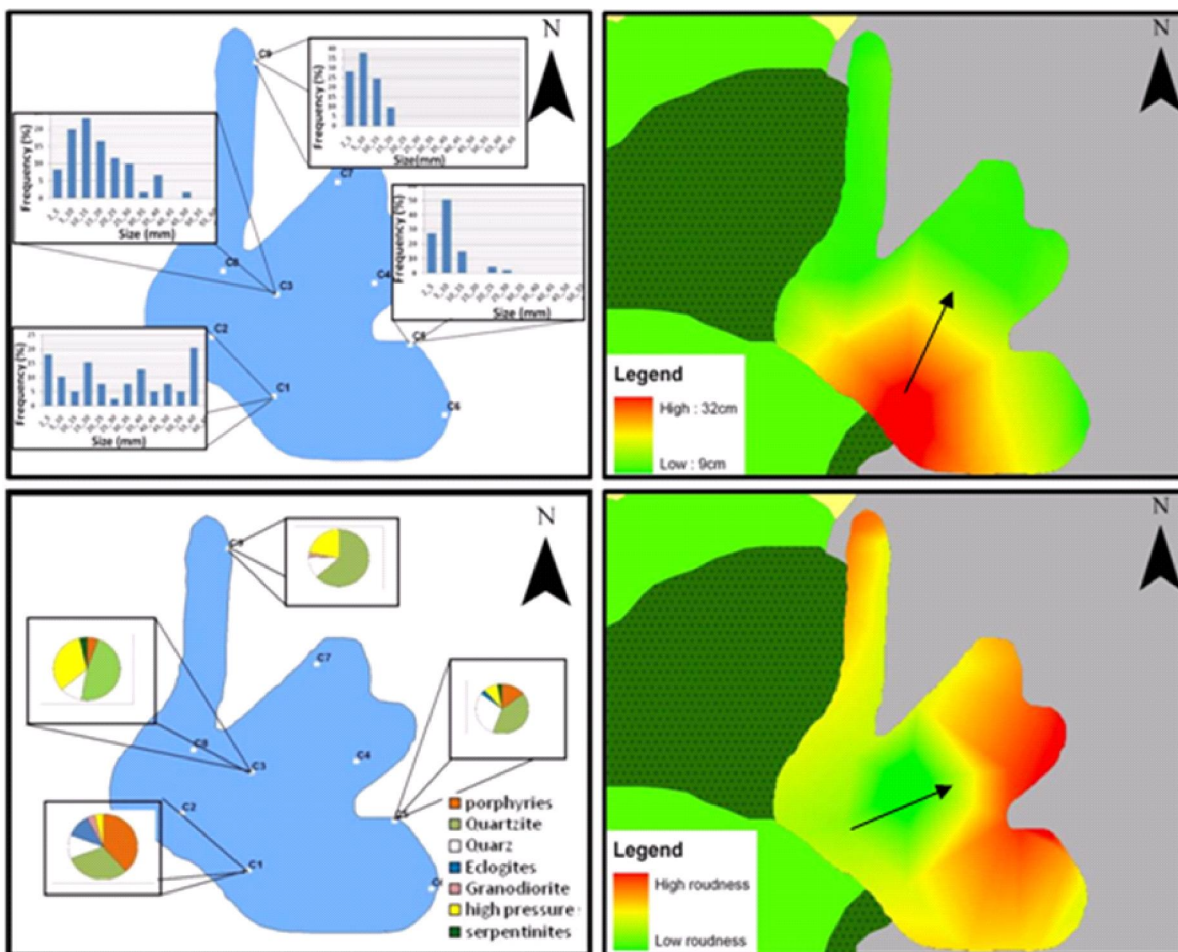


Figure 4. Distribution of the sediment properties in the studied section of the Sianamá Formation. (A) Sorting distribution histograms for some of the representative stations. (B) Size distribution integrated map. (C) Composition pie-charts from some of the representative stations. (D) Roundness distribution integrated map. The black arrow indicates the average paleoflow direction.

Eclogite and high-pressure metapelite clasts tend to be more rounded and spherical compared to the other rock types. This is either due to the fact that these rocks suffered more transport, or they reflect a particular characteristic of the source. The source of these rocks is probably a tectonic mélange (Zuluaga et al., 2008; Weber et al., 2009), and therefore we consider that the ductile deformation associated to the shearing created rounded lens shaped fragments before exposing them to the sedimentary processes. Consequently, the exposure to transport increased the roundness and sphericity of these rocks, compared to the porphyries, granodiorites, quartzites and low-grade schists, also present in the conglomerate.

6. SANDSTONE PETROGRAPHY

Three samples (SZH 01, SZH 02 and SZH 03) from the sandstone unit of the studied section were collected for petrographic analysis (Figure 1). At least three hundred points were counted following the Gazzi-Dickinson method (Gazzi, 1966; Dickinson, 1970; Ingersoll et al., 1984).

The sandstones are medium-grained rocks with highly angular fragments and poor sorting. They include mono and polycrystalline quartz, feldspar and igneous and metamorphic clasts (Figure 5). A clay matrix with carbonate cement represents over 15% of the rock.

Detrital modes are included in Table 1. The samples are classified as lithic arkose with high quartz content (Folk et al., 1974) (Figure 6-A). The abundance of quartz and lithic fragments suggests that the tectonic environment during sandstone deposition is likely to be a recycled orogen (Dickinson and Suczek, 1979; Dickinson et al., 1983; Figure 6-B). This environment is commonly related to the erosion of active orogenic belts and subduction complexes (Dickinson et al., 1983), where upper crustal rocks are deformed and rapidly exposed to erosion.

Table 1. Detrital modes of the sandstone samples. Qm (monocrystalline quartz), Qp (polycrystalline quartz), F (feldspar), P (plagioclase), Lhp (porphyritic lithic fragments), Lm (metamorphic lithic fragments).

	Qm%	Qp%	F%	Pl%	Lh%	Lm%	Otros%
SZH 01	29,5	35,8	5,2	7,4	4,8	13,6	3,7
SZH 09	25,8	31,3	12,7	5,5	6,6	14,5	3,5
SZH 21	30,6	31,7	3,1	12,6	4,8	13,1	4,1

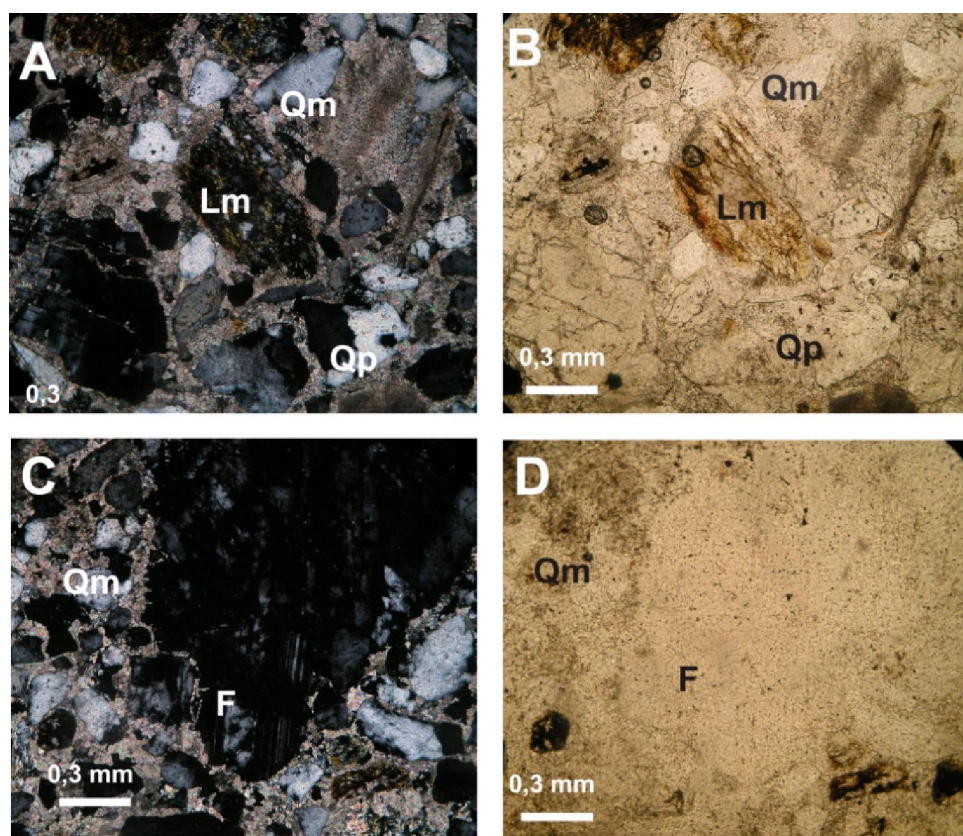


Figure 5. Representative thin sections of analyzed sandstones. Qm (monocrystalline quartz), Qp (polycrystalline quartz), F (feldspar), Lm (metamorphic lithic fragments).

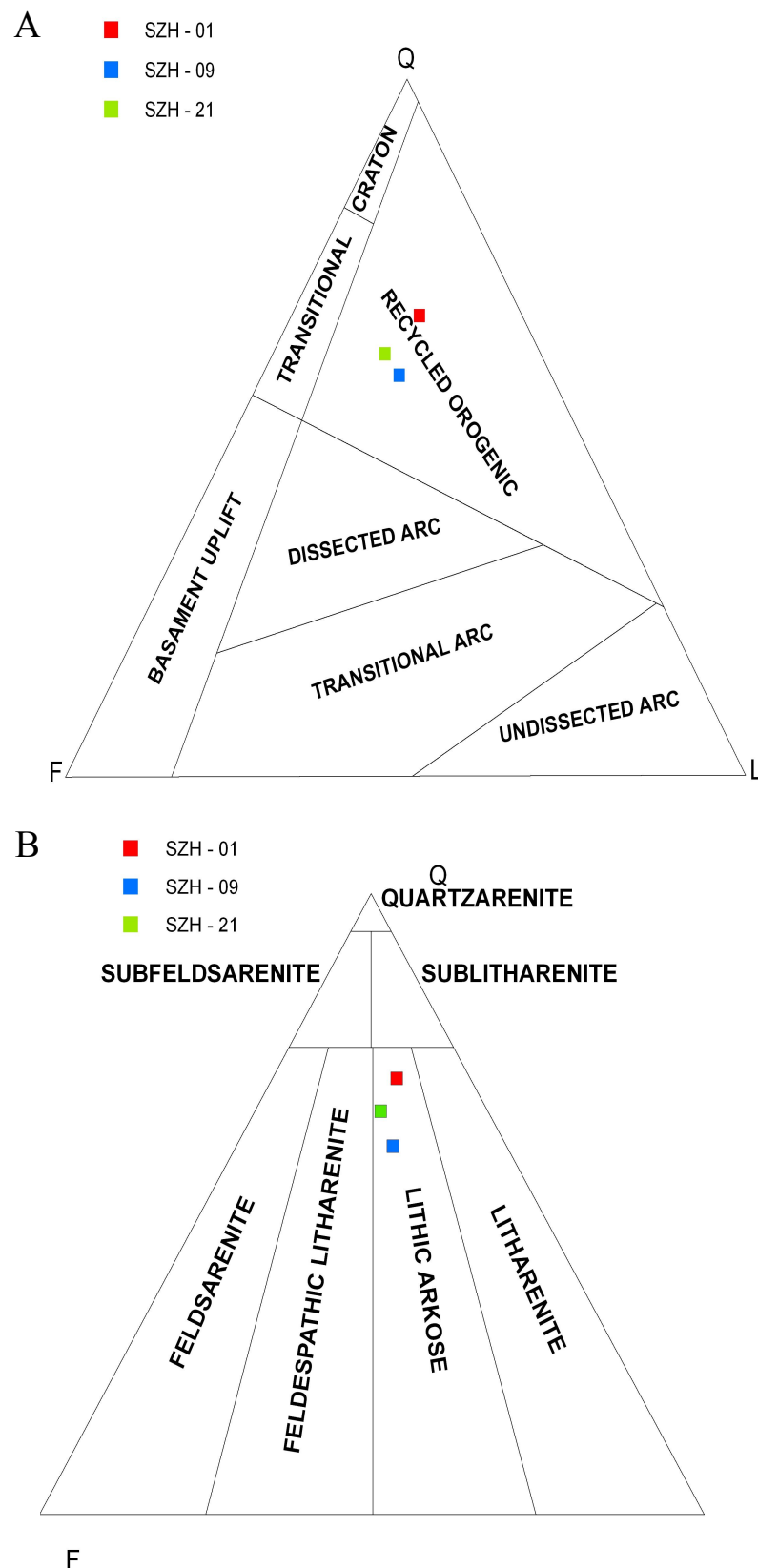


Figure 6. Three sandstone samples plotted on the sample classification QFL diagram from Folk (1974) (A) and the sandstone discrimination diagram from Dickinson (1983) (B).

7. HEAVY MINERALS

Heavy mineral suites provide important information on the sedimentary provenance (Pettijohn, 1975). The same three sandstone samples were selected for detailed heavy mineral analysis. In each section at least three hundred grains of non-opaque heavy minerals were counted. Identified minerals include epidote group minerals (zoisite, clinozoisite, epidote), garnet, amphibole, rutile, pyroxene and pyroxene (Figures 7 and 8). The heavy minerals show a similar geographic variability in relation with the composition of the rock clasts seen in the conglomerates.

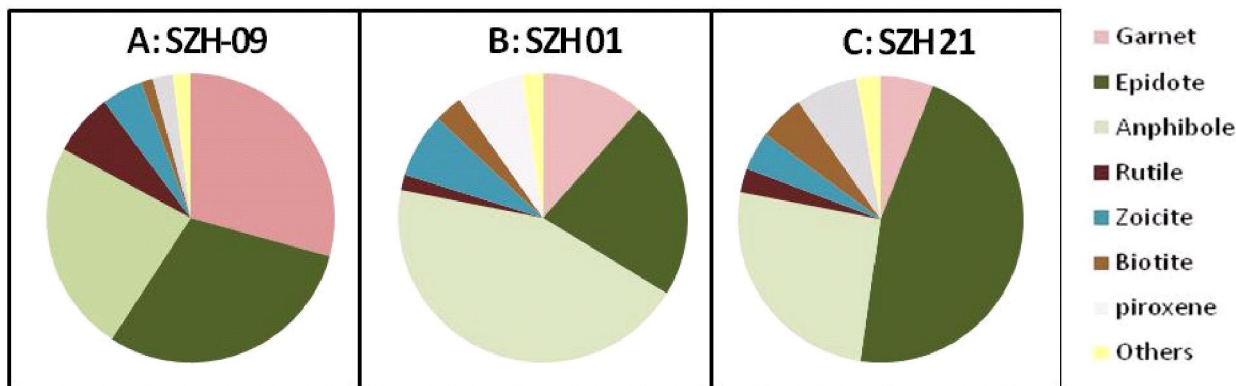


Figure 7. Heavy mineral suite for the three studied samples. (A) Sample SZH-09. (B) sample SZH-01. (C) sample SZH-21

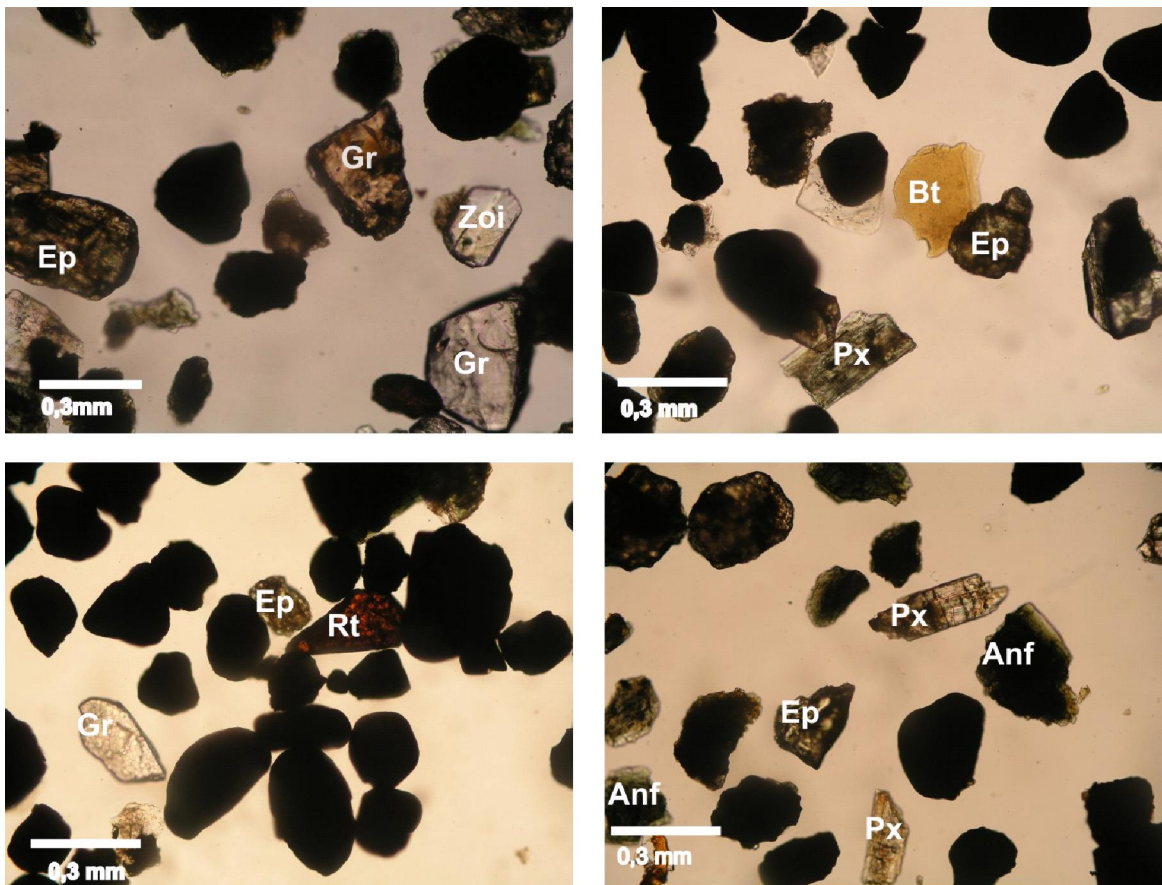


Figure 8. Heavy minerals in thin section from selected samples of the Siamaná Formation sandstones. Gr= garnet, Ep= epidote, Zoi= zoicite, Bt= biotite, Px= pyroxene, Rt= rutile, Anf= amphibole.

8. U-Pb DETRITAL ZIRCONS

One hundred and five detrital zircon grains were analyzed from sample MSZH-01. Results are presented in Table 2. Zircons younger than 1200 Ma are concordant. Older zircons are generally also concordant, but include some grains that fall outside of the Concordia (Figures 9A).

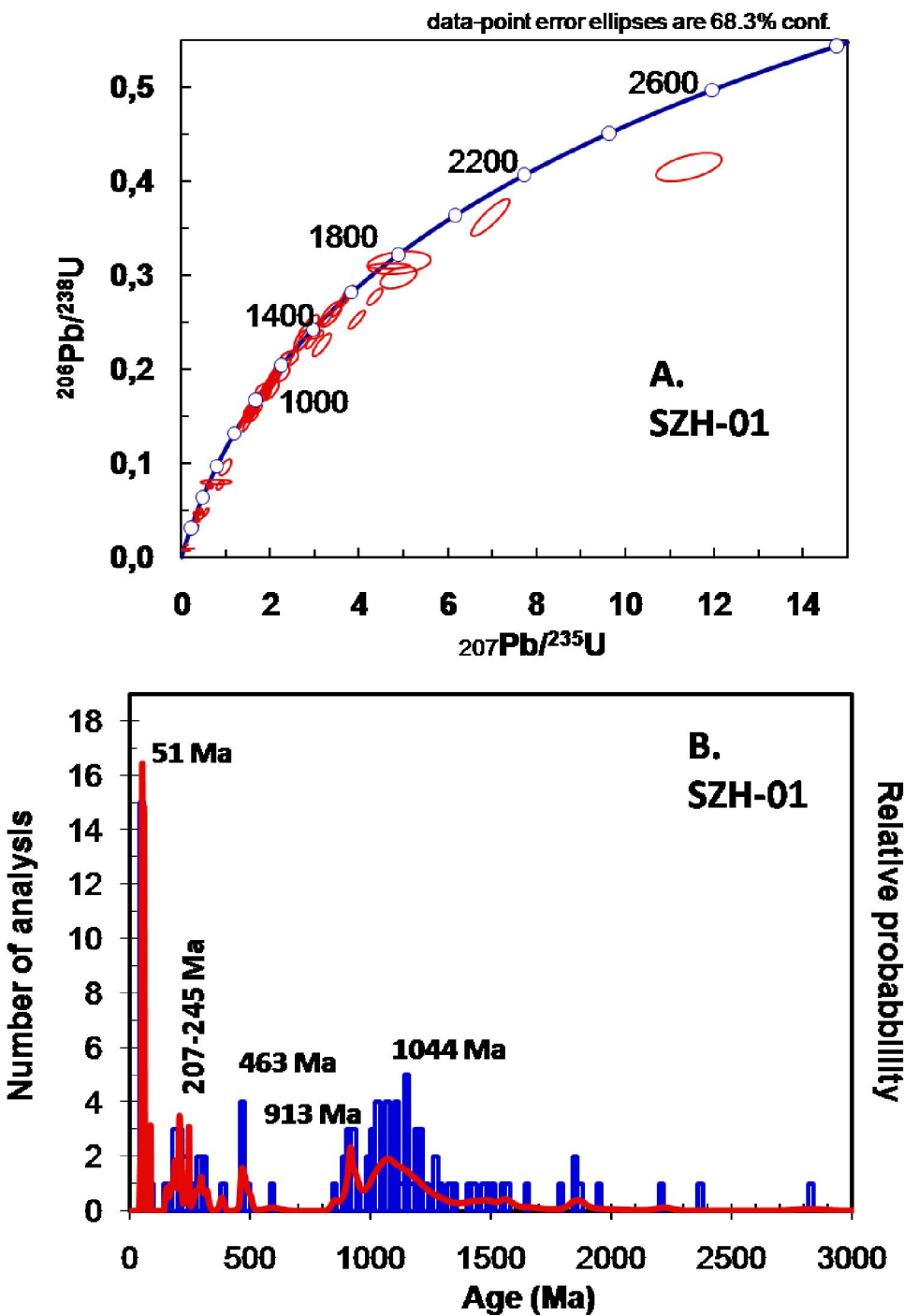


Figure 9. U/Pb detrital zircon results from sample SZH-01. (A) Concordia diagram, (B) Detrital age distribution histogram.

Table 2. U-Pb detrital zircon results from sandstone sample MSZH-01

Analysis	U (ppm)	206Pb 204Pb	U/Th	206Pb* 207Pb*	± (%)	207Pb* 235U*	± (%)	206Pb* 238U	± (%)	error corr.	206Pb* 238U*	± (Ma)	235U (Ma)	207Pb* 235U	± (Ma)	206Pb* 207Pb*	± (Ma)	Best age (Ma)	± (Ma)	Conc (%)
MSZH-1	154	4108	1,0	19,8184	14,6	0,2089	15,9	0,0300	6,3	0,40	190,7	11,9	192,6	27,9	216,1	339,2	190,7	11,9	88,2	
MSZH-3	199	27560	3,6	14,7361	1,2	1,3184	2,1	0,1409	1,7	0,81	849,8	13,6	853,8	12,1	864,3	25,4	849,8	13,6	98,3	
MSZH-4	10	570	26,8	17,2340	6,0	0,2992	6,9	0,0374	3,5	0,50	236,7	8,0	265,8	16,1	530,7	130,9	236,7	8,0	44,6	
MSZH-5	320	82240	4,2	13,3520	1,2	1,8207	2,8	0,1763	2,6	0,91	1046,8	24,6	1052,9	18,3	1065,7	23,1	1065,7	23,1	98,2	
MSZH-11	436	105968	4,0	13,3204	2,2	1,5330	6,5	0,1481	6,1	0,94	890,3	51,1	943,7	40,0	1070,5	43,6	1070,5	43,6	83,2	
MSZH-12	468	5570	8,8	16,8131	5,9	0,6306	6,2	0,0769	2,0	0,32	477,6	9,3	496,5	24,5	584,6	128,1	477,6	9,3	81,7	
MSZH-16	157	403	1,8	18,6352	6,1	0,0669	6,8	0,0090	3,0	0,44	58,0	1,7	65,8	4,3	356,9	138,5	58,0	1,7	16,3	
MSZH-7	102	3733	2,1	17,0525	26,6	0,2693	26,6	0,0333	2,3	0,08	211,2	4,7	242,2	57,5	553,8	588,9	211,2	4,7	38,1	
MSZH-8	227	435	0,6	20,1108	14,6	0,2565	14,8	0,0374	2,6	0,18	236,7	6,1	231,8	30,7	182,1	341,6	236,7	6,1	130,0	
MSZH-9	161	2070	1,4	14,2721	28,7	0,7784	28,8	0,0806	2,0	0,07	499,5	9,7	584,6	128,7	930,3	601,9	499,5	9,7	53,7	
MSZH-10	162	1028	1,7	16,5794	19,9	0,1106	20,0	0,0133	1,6	0,08	85,2	1,4	106,5	20,2	614,9	434,7	85,2	1,4	13,9	
MSZH-11	161	4438	2,0	12,4720	2,2	2,0156	2,3	0,1823	0,9	0,39	1079,6	9,1	1120,8	15,9	1201,4	42,5	1201,4	42,5	89,9	
MSZH-12	95	1153	2,6	18,1412	6,6	0,0606	6,8	0,0080	1,6	0,23	51,2	0,8	59,7	3,9	417,2	147,7	51,2	0,8	12,3	
MSZH-13	98	26290	2,7	13,0790	1,8	1,9863	5,5	0,1884	5,2	0,94	1112,8	53,2	1110,9	37,3	1107,1	36,4	1107,1	36,4	100,5	
MSZH-14	91	29878	1,2	10,2993	1,6	3,7200	3,1	0,2779	2,7	0,86	1580,7	37,6	1575,7	24,9	1569,0	29,4	1569,0	29,4	100,7	
MSZH-15	92	1133	1,7	23,9077	101,3	0,0458	101,3	0,0079	1,9	0,02	51,0	1,0	45,5	45,1	-236,9	1235,7	51,0	1,0	-21,5	
MSZH-16	100	21475	14,2	12,6633	4,0	1,8836	4,8	0,1730	2,6	0,55	1028,6	24,8	1075,3	31,6	1171,4	78,8	1171,4	78,8	87,8	
MSZH-17	20	1663	0,9	12,8464	4,0	1,6109	4,7	0,1501	2,3	0,50	901,5	19,6	974,5	29,3	1142,8	80,5	1142,8	80,5	78,9	
MSZH-18	267	4790	0,8	8,4000	4,9	4,8895	5,5	0,2979	2,6	0,46	1680,8	38,0	1800,4	46,7	1942,0	87,7	1942,0	87,7	86,6	
MSZH-19	132	26825	3,0	13,2738	1,9	1,8804	2,4	0,1810	1,5	0,63	1072,6	15,0	1074,2	16,0	1077,5	37,8	1077,5	37,8	99,5	
MSZH-20	12	1423	1,7	12,3437	5,6	1,9826	6,8	0,1775	3,9	0,58	1053,2	38,2	1109,6	46,0	1221,7	109,3	1221,7	109,3	86,2	
MSZH-21	74	18128	2,2	11,7326	3,8	2,8085	6,6	0,2390	5,4	0,82	1381,4	66,8	1357,8	49,4	1320,8	74,0	1320,8	74,0	104,6	
MSZH-22	341	5120	1,2	9,1417	6,5	4,6783	6,5	0,3102	0,6	0,10	1741,6	9,6	1763,4	54,3	1789,2	117,8	1789,2	117,8	97,3	
MSZH-23	103	355	2,1	18,6447	33,4	0,0655	33,7	0,0089	4,3	0,13	56,9	2,4	64,4	21,0	355,7	774,4	56,9	2,4	16,0	
MSZH-24	68	523	2,0	14,9738	30,4	0,0813	30,6	0,0088	3,4	0,11	56,7	1,9	79,4	23,4	831,0	648,5	56,7	1,9	6,8	
MSZH-25	117	890	1,0	17,0261	6,4	0,4951	6,8	0,0611	2,4	0,36	382,5	9,0	408,4	22,9	557,2	138,9	382,5	9,0	68,7	
MSZH-27	11	1190	1,8	9,8435	2,4	3,1628	4,3	0,2258	3,6	0,83	1312,4	42,2	1448,1	32,9	1653,4	43,8	1653,4	43,8	79,4	
MSZH-29	265	9425	2,7	13,9499	2,9	1,5312	3,5	0,1549	2,0	0,56	928,5	16,9	943,0	21,5	977,0	59,2	928,5	16,9	95,0	
MSZH-31	176	31770	2,7	13,6534	2,4	1,5370	3,0	0,1522	1,7	0,56	913,3	14,1	945,3	18,2	1020,6	49,5	913,3	14,1	89,5	
MSZH-33	567	5255	8,4	13,4035	6,2	0,9899	8,6	0,0962	6,0	0,69	592,3	33,7	698,7	43,4	1058,0	124,3	592,3	33,7	56,0	
MSZH-34	61	490	2,6	5,0078	3,5	11,4315	4,2	0,4152	2,3	0,55	2238,6	44,0	2559,0	39,6	2823,6	57,9	2823,6	57,9	79,3	
MSZH-35	273	1018	2,1	17,7080	20,1	0,3668	20,2	0,0471	2,0	0,10	296,8	5,7	317,3	55,1	471,0	448,8	296,8	5,7	63,0	
MSZH-36	196	3360	3,4	16,9443	5,9	0,3547	7,1	0,0436	3,9	0,55	275,0	10,4	308,2	18,8	567,7	128,8	275,0	10,4	48,4	
MSZH-38	820	2280	23,2	14,4877	10,7	0,4258	12,0	0,0447	5,4	0,45	282,2	14,9	360,2	36,4	899,4	221,3	282,2	14,9	31,4	
MSZH-39	395	76855	7,3	11,1399	1,5	3,0614	1,8	0,2473	1,0	0,57	1424,8	12,9	1423,1	13,5	1420,6	27,7	1420,6	27,7	100,3	
MSZH-40	43	10133	2,2	11,5711	2,6	2,7576	4,3	0,2314	3,4	0,80	1341,9	40,9	1344,1	31,7	1347,6	49,8	1347,6	49,8	99,6	
MSZH-41	117	1095	1,8	20,2869	7,1	0,0545	8,2	0,0380	4,1	0,50	51,5	2,1	53,9	4,3	161,8	166,9	51,5	2,1	31,8	
MSZH-42	136	5413	1,9	7,1737	2,0	6,9539	4,2	0,3618	3,7	0,88	1990,7	62,5	2105,6	37,0	2219,7	34,9	2219,7	34,9	89,7	
MSZH-43	131	20248	4,0	13,4380	2,6	1,7623	3,1	0,1718	1,7	0,54	1021,8	16,0	1031,7	20,2	1052,8	52,9	1052,8	52,9	97,1	
MSZH-44	18	2778	2,6	12,4307	5,6	0,5392	7,9	0,0486	5,6	0,71	306,0	16,8	437,9	28,1	1208,0	109,6	306,0	16,8	25,3	
MSZH-45	210	35575	1,9	14,4450	1,3	1,4559	1,4	0,1525	0,6	0,45	915,1	5,5	912,3	8,6	905,5	26,3	915,1	5,5	101,1	
MSZH-46	150	33970	0,6	14,2489	1,9	1,4838	3,4	0,1533	2,8	0,84	919,6	24,3	923,8	20,6	933,7	38,2	919,6	24,3	98,5	
MSZH-48	464	1303	12,1	15,5503	3,1	0,6774	3,7	0,0764	2,0	0,53	474,6	9,0	525,2	15,2	751,7	66,4	474,6	9,0	63,1	
MSZH-49	480	7398	1,1	8,7643	1,6	4,3608	2,6	0,2772	2,0	0,77	1577,2	27,7	1704,9	21,3	1865,7	29,6	1865,7	29,6	84,5	
MSZH-50	66	16043	1,6	13,7141	2,8	1,5942	4,1	0,1586	2,9	0,72	948,8	25,9	967,9	25,5	1011,6	57,6	1011,6	57,6	93,8	
MSZH-51	296	42798	1,1	8,8267	1,5	3,9498	3,0	0,2529	2,6	0,87	1453,2	33,8	1623,9	24,2	1852,9	26,6	1852,9	26,6	78,4	
MSZH-52	65	7288	1,1	13,9653	4,2	1,5651	4,8	0,1585	2,3	0,48	948,6	20,2	956,5	29,6	974,8	85,4	948,6	20,2	97,3	
MSZH-53	39	8885	2,1	12,0593	5,3	2,4195	5,9	0,2116	2,5	0,43	1237,4	28,5	1248,4	42,4	1267,4	104,0	1267,4	104,0	97,6	
MSZH-54	247	28618	1,5	10,7255	1,4	3,2778	2,3	0,2550	1,8	0,78	1464,1	23,3	1475,8	17,7	1492,7	26,8	1492,7	26,8	98,1	
MSZH-55	87	688	1,8	20,2170	7,1	0,0544	7,9	0,0080	3,4	0,43	51,2	1,7	53,8	4,1	169,8	166,0	51,2	1,7	30,2	
MSZH-56	192	28828	2,4	13,9450	2,9	1,5302	3,4	0,1548	1,7	0,50	927,6	14,5	942,6	20,6	977,7	59,3	927,6	14,5	94,9	
MSZH-57	97	18378	3,0	12,8034	2,0	2,1066	2,4	0,1956	1,3	0,55	1151,7	13,7	1151,0	16,3	1149,5	39,4	1149,5	39,4	100,2	
MSZH-58	24	4100	1,3	13,4151	2,0	1,6787	4,8	0,1633	4,4	0,91	975,2	39,4	1000,5	30,4	1056,2	39,4	1056,2	39,4	92,3	
MSZH-59	238	3323	0,8	20,2185	9,3	0,1837	9,8	0,0269	3,3	0,33	171,3	5,5	171,2	15,5	169,7	216,4	171,3	5,5	101,0	
MSZH-60	138	26080	2,1	13,1120	2,1	1,9747	2,7													

Analysis	U (ppm)	Best																	
		206Pb	U/Th	206Pb*	±	207Pb*	±	206Pb*	±	error	206Pb*	±	207Pb*	±	206Pb*	±	age (Ma)	± (Ma)	Conc (%)
		204Pb		207Pb*	(%)	235U*	(%)	238U	(%)	corr.	238U*	(Ma)	235U	(Ma)	207Pb*	(Ma)	206Pb*	(Ma)	± (Ma)
MSZH1-61	10	1730	0,1	13,6403	1,6	1,6123	2,5	0,1595	2,0	0,78	954,0	17,4	975,0	15,7	1022,6	31,8	1022,6	31,8	93,3
MSZH1-62	40	7008	0,7	14,4584	3,2	1,4801	4,0	0,1552	2,3	0,58	930,1	20,1	922,3	24,1	903,6	66,4	930,1	20,1	102,9
MSZH1-63	189	1375	2,1	18,5623	13,2	0,0688	13,6	0,0093	3,4	0,25	59,4	2,0	67,5	8,9	365,7	298,8	59,4	2,0	16,2
MSZH1-64	60	593	2,0	19,4540	39,0	0,0572	39,2	0,0081	4,1	0,10	51,8	2,1	56,5	21,5	259,0	928,0	51,8	2,1	20,0
MSZH1-65	116	390	1,4	9,8312	18,8	0,1282	18,9	0,0091	2,3	0,12	58,6	1,3	122,4	21,8	1655,7	350,8	58,6	1,3	3,5
MSZH1-66	55	1373	0,8	16,7349	29,3	0,2490	30,0	0,0302	6,7	0,22	192,0	12,7	225,8	60,9	594,7	647,5	192,0	12,7	32,3
MSZH1-68	25	4098	3,1	10,8681	1,8	2,9507	3,6	0,2326	3,1	0,87	1348,0	37,6	1395,0	27,0	1467,6	33,4	1467,6	33,4	91,9
MSZH1-69	163	313	2,8	6,5351	30,9	0,2020	31,0	0,0096	1,5	0,05	61,4	0,9	186,8	52,9	2379,9	541,6	2379,9	541,6	2,6
MSZH1-70	185	13305	0,9	11,2096	6,0	2,9254	6,2	0,2378	1,4	0,22	1375,4	16,7	1388,5	46,6	1408,6	115,1	1408,6	115,1	97,6
MSZH1-71	135	7073	1,4	12,9081	3,0	1,9003	3,7	0,1779	2,1	0,58	1055,5	20,8	1081,2	24,7	1133,4	60,4	1133,4	60,4	93,1
MSZH1-72	88	16343	2,4	14,5612	2,1	1,4136	3,3	0,1493	2,6	0,78	897,0	21,7	894,7	19,7	889,0	42,8	897,0	21,7	100,9
MSZH1-73	128	21928	5,1	13,0384	2,0	1,9119	3,0	0,1808	2,2	0,73	1071,3	21,3	1085,2	19,7	1113,3	40,1	1113,3	40,1	96,2
MSZH1-76	50	2418	0,9	13,3630	4,3	1,6268	4,8	0,1577	2,2	0,45	943,8	19,1	980,6	30,3	1064,1	86,6	1064,1	86,6	88,7
MSZH1-77	164	16123	2,5	13,8817	1,9	1,6782	2,3	0,1690	1,3	0,57	1006,4	12,0	1000,3	14,5	987,0	38,3	987,0	38,3	102,0
MSZH1-78	323	22325	4,6	13,4302	1,6	1,7346	2,6	0,1690	2,0	0,78	1006,4	18,7	1021,4	16,5	1054,0	32,3	1054,0	32,3	95,5
MSZH1-79	379	1690	7,3	14,6834	8,6	0,3642	8,7	0,0388	0,8	0,09	245,3	1,8	315,3	23,5	871,7	179,2	245,3	1,8	28,1
MSZH1-80	55	375	2,1	10,0034	60,4	0,0975	60,6	0,0071	5,6	0,09	45,5	2,5	94,5	54,8	1623,4	1256,6	45,5	2,5	2,8
MSZH1-81	124	13290	4,2	12,3686	3,4	2,3954	3,6	0,2149	1,2	0,35	1254,8	14,1	1241,2	25,6	1217,8	66,0	1217,8	66,0	103,0
MSZH1-82	791	22280	3,5	12,4870	1,8	1,7482	2,7	0,1583	2,0	0,75	947,5	18,0	1026,5	17,6	1199,1	35,4	1199,1	35,4	79,0
MSZH1-83	130	450	2,4	21,7833	17,3	0,0549	17,5	0,0087	2,9	0,17	55,7	1,6	54,3	9,3	-7,3	419,2	55,7	1,6	-767,7
MSZH1-83A	630	50510	3,7	13,6614	1,4	1,7352	2,3	0,1719	1,8	0,78	1022,7	17,2	1021,7	15,0	1019,4	29,2	1019,4	29,2	100,3
MSZH1-85	266	358	1,9	17,1436	4,0	0,1948	5,3	0,0242	3,4	0,64	154,3	5,2	180,8	8,7	542,2	88,2	154,3	5,2	28,5
MSZH1-86	71	8978	2,9	13,0719	1,9	1,6417	2,9	0,1556	2,2	0,76	932,5	19,4	986,4	18,4	1108,2	37,5	1108,2	37,5	84,1
MSZH1-87	265	9985	3,7	12,0128	1,8	2,3918	2,1	0,2084	1,1	0,54	1220,2	12,5	1240,1	15,0	1274,9	34,4	1274,9	34,4	95,7
MSZH1-88	535	7810	1,0	19,3032	6,0	0,2326	6,1	0,0326	1,3	0,21	206,6	2,6	212,4	11,8	276,8	137,8	206,6	2,6	74,6
MSZH1-89	36	5143	5,4	13,7989	1,7	1,6006	2,4	0,1602	1,7	0,69	957,8	14,7	970,4	14,9	999,1	35,2	999,1	35,2	95,9
MSZH1-91	243	3013	1,2	17,9510	8,1	0,2513	8,5	0,0327	2,6	0,31	207,5	5,4	227,6	17,3	440,7	180,2	207,5	5,4	47,1
MSZH1-92	359	31453	2,6	10,3623	1,3	3,5627	3,2	0,2678	3,0	0,92	1529,4	40,6	1541,3	25,7	1557,6	23,8	1557,6	23,8	98,2
MSZH1-93	427	6753	2,3	12,8414	1,5	2,0121	1,7	0,1874	0,9	0,53	1107,2	9,3	1119,6	11,7	1143,6	29,2	1143,6	29,2	96,8
MSZH1-96	227	5500	2,2	17,0786	24,1	0,2376	24,2	0,0294	2,1	0,09	187,0	3,9	216,4	47,1	550,5	532,4	187,0	3,9	34,0
MSZH1-97	681	6408	12,4	15,9711	6,2	0,6453	6,3	0,0747	1,2	0,18	464,7	5,2	505,6	25,2	695,1	132,5	464,7	5,2	66,8
MSZH1-98	147	6093	3,4	18,0883	10,5	0,3872	10,8	0,0508	2,6	0,24	319,4	8,0	332,3	30,7	423,7	235,6	319,4	8,0	75,4
MSZH1-100	64	4960	3,5	11,9358	4,6	2,2603	5,3	0,1957	2,7	0,50	1152,0	28,4	1200,0	37,6	1287,5	89,9	1287,5	89,9	89,5
MSZH1-101	110	403	2,3	18,6196	43,5	0,0655	43,7	0,0088	4,3	0,10	56,7	2,4	64,4	27,3	358,8	1026,4	56,7	2,4	15,8
MSZH1-102	117	425	3,8	17,9568	37,4	0,0680	37,5	0,0088	3,5	0,09	56,8	2,0	66,8	24,3	440,0	859,8	56,8	2,0	12,9
MSZH1-103	100	17088	1,1	8,8241	9,3	4,8982	9,6	0,3135	2,7	0,27	1757,8	40,8	1801,9	81,5	1853,4	167,9	1853,4	167,9	94,8
MSZH1-106	280	1145	1,2	12,2537	5,1	0,8915	6,5	0,0766	4,0	0,62	475,6	18,5	630,9	30,6	1236,2	99,9	475,6	18,5	38,5
MSZH1-107	53	10623	0,9	12,8063	2,9	1,8874	4,1	0,1753	3,0	0,72	1041,3	28,4	1076,7	27,3	1149,1	57,0	1149,1	57,0	90,6
MSZH1-108	211	41073	2,0	13,5896	1,5	1,6180	3,7	0,1595	3,4	0,92	953,8	30,5	977,2	23,5	1030,1	30,0	1030,1	30,0	92,6
MSZH1-109	349	67523	4,4	12,8610	1,3	1,9427	1,9	0,1812	1,3	0,70	1073,6	13,0	1095,9	12,6	1140,6	26,7	1140,6	26,7	94,1
MSZH1-110	255	60888	5,6	14,5098	1,4	1,4196	3,3	0,1494	3,0	0,91	897,6	25,2	897,2	19,7	896,3	28,1	897,6	25,2	100,1
MSZH1-111	185	35848	6,9	12,3655	2,0	2,1678	5,9	0,1944	5,5	0,94	1145,2	58,1	1170,8	41,0	1218,3	39,7	1218,3	39,7	94,0
MSZH1-112	128	22215	2,3	13,2500	1,2	1,7945	3,0	0,1724	2,8	0,92	1025,6	26,4	1043,5	19,8	1081,1	24,2	1081,1	24,2	94,9
MSZH1-113	149	29485	1,9	13,1707	2,0	1,6860	3,6	0,1611	3,0	0,83	962,6	26,7	1003,3	22,9	1093,1	40,1	1093,1	40,1	88,1
MSZH1-114	228	30655	2,8	13,5550	2,2	1,6108	6,2	0,1584	5,8	0,93	947,6	51,1	974,4	38,9	1035,3	44,5	1035,3	44,5	91,5
MSZH1-115	149	28745	3,9	12,5442	1,5	2,0642	6,2	0,1878	6,0	0,97	1109,4	61,5	1137,0	42,5	1190,0	28,7	1190,0	28,7	93,2
MSZH1-116	106	27305	2,2	10,5829	3,4	3,3726	4,8	0,2589	3,4	0,71	1484,0	45,3	1498,1	37,9	1518,0	64,5	1518,0	64,5	97,8
MSZH1-117	72	14215	4,0	12,5896	3,0	2,1408	5,1	0,1955	4,1	0,81	1151,0	43,6	1162,1	35,5	1182,9	59,5	1182,9	59,5	97,3
MSZH1-118	128	570	2,4	15,2539	11,3	0,0750	13,3	0,0083	7,0	0,52	53,2	3,7	73,4	9,4	792,2	238,6	53,2	3,7	6,7
MSZH1-119	54	10200	2,6	13,6658	4,2	1,8011	4,9	0,1785	2,5	0,51	1058,8	24,2	1045,8	32,0	1018,8	85,8	1018,8	85,8	103,9
MSZH1-120	63	10783	1,3	13,5654	3,1	1,5923	3,5	0,1567	1,6	0,46	938,2	14,0	967,2	21,7	1033,7	62,3	1033,7	62,3	90,8

The major age distribution peak comprises 10 zircons with an age of approximately 50 Ma. (Figure 9B) and also represents the youngest age recorded for this sample. The rest of the zircons show five different age distribution peaks at 207 Ma, 245 Ma, 463 Ma, 913 Ma and 1044 Ma (Figure 9B). The Mesozoic and Grenvillian peaks are included in relatively continuous age intervals, which suggest a highly mixed and recycled source of zircons, probably linked to sediments or metasediments.

Single grains with Meso and Paleoproterozoic and Archean ages were also analyzed. These zircons suggest that there are in fact older ages, however they do not comprise a statistically well defined particular population (Gehrels et al., 2006). Young Eocene zircons limit sedimentation to this time span. With the exception of three grains, all of the analyzed zircons have U/Th ratios < 12 which is typical of magmatic zircons (Rubatto, 2002). The other three grains include Permian (2) and Grenvillian age with higher ratios that must be related to a metamorphic source.

9. DISCUSSION AND CONCLUSIONS

9.1 Provenance of the Siamaná siliciclastics

Bad sorting, low roundness, presence of non-altered feldspars and biotite, and an unstable heavy mineral fraction suggest that conglomeratic and sandy materials deposited in the Siamaná Formation were not exposed to long transport and derived from a very proximal source.

Sorting, size and clast composition have shown that the conglomerates were derived directly from a source located to the south to southeast. Igneous (porphyries and granodiorites) and low-grade schist clasts and polycrystalline quartz in the conglomerate and the sandstones of the studied siliciclastic sequence of the Siamaná Formation can be correlated to the erosion of the immediately adjacent Jarara and Etpana Formations and the Parashi Stock. The presence of amphibole and biotite can be also related to the erosion of the Parashi Stock and Jarara or Etpana Formations, and their presence, together with additional unstable pyroxene, clearly indicate short travel distances and fast deposition, that result in lack of transient weathering. U-Pb detrital zircon ages can also be compared to the adjacent Parashi Stock with ages of approximately 50 Ma (Cardona, Weber and Valencia unpublished data). The older ages are similar to the detrital ages recorded by the metasedimentary rocks of the Etpana Formation and the high-pressure metamorphic clasts (Weber et al., 2009).

Tectonic setting sandstone discrimination diagrams after Dickinson et al. (1983) and Suczek et al. (1983) show that the samples fall within the field of a recycled orogen. Normally tectonic provenance patterns are more related to the composition of the source area than the specific basin or source area tectonic setting (Augustsson and Bahlburg, 2003). It is therefore suggested that pre-Oligocene magmatic and metamorphic rocks filled the basin, such as those found in the Serranía de Jarara.

Unfortunately the source of the high-pressure metamorphic fragments remains not found (Lockwood, 1965; Weber et al., 2007; 2009). However, their limited spatial exposure and roundness suggest that they were probably derived from the Cretaceous tectonic mélange postulated by Weber et al. (2007, 2009) and Zuluaga et al. (2008), where the high-pressure rocks are most likely to be minor blocks in a schistose matrix (Weber et al., 2007, 2009; Zuluaga et al., 2008, Zapata, 2005). And have been rounded during shearing.

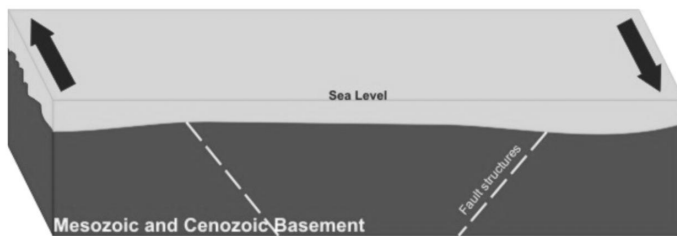
9.2 Tectonosedimentary implications

In general, the Siamaná Formation has been considered of Middle to Late Oligocene in age (Renz, 1960; Lockwood, 1965). The presence of marine fossils of shallow environments described by Rollins (1965) and of carbonate cement in the conglomerate and sandstone sequence suggests that the studied section was deposited in a shallow marine environment, and that the relatively thick and coarse conglomerate deposits are related to a marine type fan delta (McPherson et al., 1987).

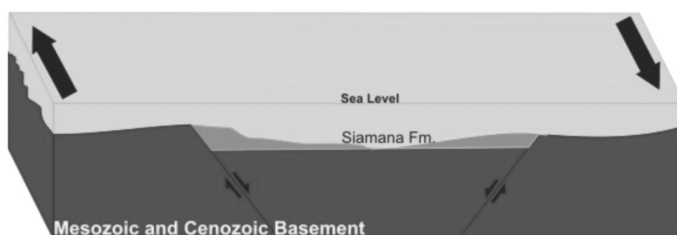
Tectonic reconstructions have shown that following the Paleogene collision and frontal convergence with the northern margin of Colombia, the Caribbean plate changed to a relative eastern migration that allowed the formation and transition to several back-arc and pull-apart basins on the margins (Muessig, 1984; Macellari, 1995; Pindell et al., 1998; Ramirez, 2006; Gorney et al., 2007; Vence, 2008; Pindell and Keenan, 2009). It is therefore suggested that the conglomerate described here is related to the opening of a pull-apart basin during the Oligocene that caused the formation of a basin and the simultaneous proximal uplift or push-up of blocks such as the adjacent Serranía de Jarara (Figures 10A and 10B). Fan deltas derived from this uplifted block were deposited in shallow water environments within adjacent pull-apart basins. The continuous subsidence and opening of these basins may be responsible for the marine transgression, represented by the deep marine sediments of the Uitpa Formation (Rollins, 1960, in Hall and Cediel, 1971; Lockwood, 1965) (Figure 10C).

Finally, the presence of rock clasts and zircons from the Eocene Parashi Stock (ca. 50-46 Ma) suggest that following the emplacement of this granitoid, there was a major post 50 Ma unroofing event, which could include exhumation related to the basin formation, which is common in extensional settings (Ring et al., 1999; Horton and Schmitt, 1998).

A) Late Eocene



B) Early Oligocene - Middle Oligocene



C) Late Oligocene

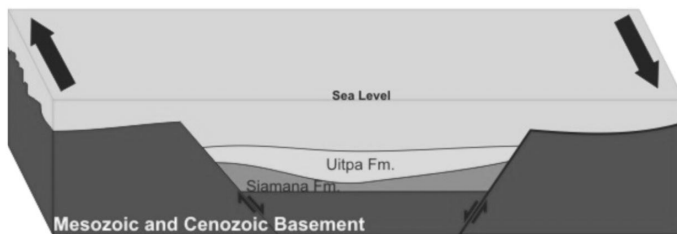


Figure 10. Simplified model for the formation and filling for pull-apart basins in the NW margin of South America. (A) The first stage before the breakup of the basement, (B) Sintectonic filling of the basin and Siamaná Formation deposition and (C) Subsidence of the basin and deposition of the Uitpa Formation.

ACKNOWLEDGEMENTS

Oscar Talavera is acknowledged for discussions and encouragement during field work. The hospitality and help of the LaserChron staff is sincerely acknowledged. Continuous help from Oscar Jaramillo of the Petrography Laboratory, Universidad Nacional de Colombia is greatly appreciated. This research was funded by the Universidad Nacional de Colombia through DIME grant 30805975. Funding for the Arizona LaserChron Center is provided by National Science Foundation grant EAR-0443387. This is a contribution to Project 546 of the International Geological Correlation Program "Subduction zones of the Caribbean".

REFERENCES

- Álvarez, W., 1967. Geology of the Simarua and Carpintero area, Guajira Peninsula, Colombia. Ph.D. thesis. Princeton University, 147 P.
- Arredondo, L.F., 2005. Caracterización de las ultramafitas y rocas asociadas de la Serranía de Jarara y su relación con las rocas del Cabo de la Vela y de la Serranía de Carpintero, Guajira-Colombia. Tesis de grado, Universidad Nacional de Colombia, 34 P.
- Augustsson, C., Bahlburg, H., 2003. Active or passive continental margin? Geochemical and Nd isotope constraints of metasediment in the backstop of a pre-Andean accretionary wedge in southernmost Chile ($46^{\circ}30' - 48^{\circ}30'S$). In McCann, T., Saintott, A (eds) Tracing tectonic deformation using the sedimentary record. Geological Society of London, Special Publications, 208, pp. 253-268.
- Boggs, S., 2009. Petrology of Sedimentary Rocks. Cambridge University, 2nd Edition, 621 P.
- Cardona, A., Weber, M., Cordani, U., Wilson, R., Gomez, J., 2007. Evolución tectono-magmática de las rocas maficas-ultramáficas del Cabo de la Vela y el Stock de Parashi, Península de la Guajira: registro de la evolución orogénica Cretácica-Eocena del norte de Suramérica y el Caribe. XI Congreso Colombiano de Geología. Bucaramanga, Agosto, pp. 14-17.
- Cardona-Molina, A., Cordani, U., MacDonald, W., 2006. Tectonic correlations of pre-Mesozoic crust from the northern termination of the Colombian Andes, Caribbean region. Journal of South American Earth Sciences, 21, pp. 337-354.
- Dickinson, W. R. 1970. Interpreting detrital modes of graywacke and arkose. Journal of Sedimentary Petrology, pp. 695-707.
- Dickinson, W. R., Suczek, C.A., 1979. Plate tectonics and sandstones compositions. American Association of Petroleum Geologists, pp. 2164-2182.
- Dickinson, W.R., Beard, L.S., Brakenridge, G.R., Erjavec, J.L., Ferguson, Inman, K.F., Kneppe, R.A. Lindberg, F.A. and Ryberg, P.T., 1983. Provenance of North American Phanerozoic sandstones in relation to tectonic setting. Geological Society of America, 94, pp. 222-235.
- Folk, R.L., Andrews, P.B. and Lewis, D.W. 1974. Detrital sedimentary rock classification and nomenclature for use in New Zealand. New Zealand Journal of Geology and Geophysics, 13, pp. 937-968.
- García-Casco, A., Cardona, A. and Valencia, V.A., 2009. Pressure temperature and time constrains for high-pressure metasedimentary rocks from northernmost Colombia - Caribbean region. III Cuban Convention in Earth Sciences. Workshop 775 "Subduction Zones of the Caribbean", pp. 13-25.
- Gazzi, P. 1966. Le arenarie del flysch sopracretaceo dell'Appennino modenese; Correlazioni con il flysch di Monghidoro. Mineralogie e Petrografia, pp. 69-97.
- Gehrels, G., Valencia, V., and Pullen, A., 2006. Detrital zircon geochronology by Laser-Ablation Multicollector

- ICPMs at the Arizona LaserChron Center. In Olszewski, T.D. (Ed), Geochronology Emerging opportunities, Special Publication Paleontological Society, 12, pp. 67-76.
- Gehrels, G., Valencia, V., and Ruiz, J., 2008. Enhanced precision, accuracy, efficiency, and spatial resolution of U-Pb ages by laser ablation-multicollector-inductively coupled plasma-mass spectrometry, *Geochemistry Geophysics Geosystems*, 9, Q03017, doi:10.1029/2007GC001805).
- Gorney, D., Escalona, A., Mann, P., Magnani, B., and Bolivar Study Group, 2007, Chronology of Cenozoic tectonic events in western Venezuela and the Leeward Antilles based on integration of offshore seismic reflection data and on land geology. *AAPG Bulletin*, 91, pp. 653 ? 684.
- Green, D. H., Lockwood, J. P., Kiss, E. 1968. Eclogite and almandine-quartz rock from the Guajira Peninsula, Colombia, South America. *The american mineralogist*, 23. pp. 1320-1335.
- Hall, M. y Cediel, F. 1971. Sedimentos marinos terciarios y recientes de la Península de. U. Nal., Geol. Col., 8, pp. 63-77.
- Horton, B.K., and Schmitt, J.G., 1998, Development and exhumation of a Neogene sedimentary basin during extension, Nevada, *Geological Society of America Bulletin*, 110, pp. 163-172.
- INGEOMINAS. 1997. Atlas Geológico Digital de Colombia. Versión 1.0. Memoria Técnica. 252 P.
- Ingersoll, R.V., Bullard, T.F., Ford, R.D., Grimm, J.P., and Pickle, J.D. 1984. The effect of grain size on detrital modes: A test of the Gazzi-Dickinson point counting method. *Journal of Sedimentology Petrology*, pp. 103-116.
- Lockwood, J. P. 1965. Geology of the Serranía de Jarara area, Guajira Peninsula, Colombia. s.l. : Tesis de Doctorado, Universidad de Princeton, 267 P.
- Ludwig, K.J., 2003. Isoplot 3.0. Berkeley Geochronology Center Special Publication. 4, 70 p.
- MacDonald, W. 1964. Geology of the Serranía de Macuira area, Guajira Peninsula, Colombia. Ph. D. Thesis. Princeton University, 167 P.
- Macellari, C. E. 1995. Cenozoic sedimentation a tectonics of the southwestern Caribbean pull-apart basin Venezuela and Colombia. in A. J. Takard, R. Suarez S, an H. J. Welsink, *Petroleum Basins of South America*, AAPG, 6.2, pp. 757 - 780.
- McPherson, J. G., Shanmugam, G., and Moiola, R. J., 1987. Fan-deltas and braid deltas: Varieties of coarse-grained deltas. *Gological society of America Bulletin*, 99, pp. 331-340.
- Montes, C., Hatcher, R.D., and Restrepo-Pace, P., 2005, Tectonic reconstruction of the northern Andean blocks. Oblique convergence and rotations derived from the kinematics of the Piedras-Girardot area, Colombia. *Tectonophysics*, 399, pp. 221-250.
- Muessig, K. W. 1984. Structure and Cenozoic tectonics of the Falcón Basin, Venezuela, and adjacent areas. In: Bonini, W. E., Hargraves, R. B., Shagam, R. (Eds.) *The Caribbean-South American plate boundary and regional tectonics*. Geological Society of America Memoir, 162, pp. 217-230.
- Pettijhon, F. J. 1975. *Sedimentary rocks*. 3r Ed., Harper and Row, pp. 628.
- Pindell, J. L. 1993. Evolution of the Gulf of Mexico and the Caribbean, in S.K. Donovan. s.l. : University of the West Indies Publisher's Association *Caribbean Geology, An Introduction*. pp. 13-39.
- Pindell, J., Kennan, L., Maresch,W. V., Stanek, K. P., Draper, G. and Higgs, R. 2005. Plate-kinematics and crustal dynamics of circum-Caribbean arc-Tectonic controls on basin development in Proto-Caribbean. s.l. : In: Avé Lallement, H. G. & Sisson, V. B. (eds) *Caribbean-South AmericanPlate Interactions*, Venezuela. Geological Society of America, *Special Papers*, 394, pp. 7-52.
- Pindell, J. L., Higgs, R. and Dewey, J. F. 1998. Cenozoic palinspastic reconstruction, paleogeographic evolution, and

- hydrocarbon setting of the northern margin of South America. In: Pindell, J. L. and Drake, C. L. (eds) Paleogeographic Evolution and Non-glacial Eustasy, northern South America. SEPM (Society for Sedimentary Geology), Special Publication, 58, pp. 45-86.
- Pindell, J., and Kennan, L., 2009. Tectonic evolution of the Gulf of Mexico, Caribbean and northern South America in the mantle reference frame: an update, in James, K., Lorente, M. A., and Pindell, J. eds., The geology and evolution of the region between North and South America. Geological Society of London Special Publication. In press.
- Rámirez, V., 2006. Geological setting and hydrocarbon occurrences, Guajira basin, offshore northern Colombia. AAPG Annual meeting, Houston. Search and discovery, article #10116.
- Toussaint, J. F., 1996. Evolución geológica de Colombia. Cretácico. U. Nal., 3, pp.1-277.
- Renz, O. 1960. Geología de la parte sureste de la Península de La Guajira (República de Colombia), Venezuela.ween North and South America. Geological Society of London Special Publication, 3, pp. 317-349
- Ring, U., Brandon, M.T., Willett, S., and Lister, G. 1999. Exhumation Processes: Normal Faulting, Ductile Flow, and Erosion, Geological Society of London Special Publication, 154, pp. 1-27.
- Rollins, J. F. 1965. Stratigraphy and structure of the Guajira Peninsula, northwestern Venezuela and northeastern Colombia. Univ. Nebraska Studies, New Ser., 30, pp. 1-1102.
- Rubatto, D., 2002. Zircon trace element geochemistry: partitioning with garnet and the link between U-Pb ages and metamorphism: Chemical Geology, 184, pp. 123-138.
- Stacey, J. S., and Krammers, J. D., 1975. Approximation of terrestrial lead isotope evolution by a two stage model. Earth and Planetary Science Letters, 26, pp. 207-221
- Vence, E.M., 2008. Subsurface structure, stratigraphy, and regional tectonic controls of the of the Guajira margin of northern Colombia. M.Sc. Thesis, Texas University, 11 P.
- Villamil, T., 1999. Campanian-Miocene tectonostratigraphy, depocenter evolution and basin development of Colombia and Western Venezuela. Palaeogeography, Paleoclimatology, Paleoecology, 153, pp. 239-275.
- Weber, M., Cardona, A., Wilson, R., Gómez-Tapias, J., and Zapata, G., 2007. Química Mineral de las rocas de alta presión-Facies Eclogita, de la Península de la Guajira, Colombia. Boletín de Geología 29, 31-39.
- Weber, M. B. I., Cardona, A., Paniagua, F., Cordani, U., Sepúlveda, L, and WILSON, R, 2009. The Cabo de la Vela mafic-ultramafic complex, Northeastern Colombian Caribbean region - A record of multi stage evolution of a Late Cretaceous intra-oceanic arc. Special Publication Geological Society of London, 328, pp. 549-568.
- Weber, M. B., Cardona, A., Valencia, V., García-Casco, A., Tobón, M., and Zapata, S. 2010. U/Pb detrital zircon provenance from Late Cretaceous metamorphic units of the Guajira Peninsula, Colombia: tectonic implications on the collision between the Caribbean arc and the South American margin. Journal of South American Earth Sciences. In press.
- Zapata, G. 2005. Análisis petrográfico y química mineral de las rocas de alta presión de la Serranía de Jarara: La Guajira y sus implicaciones tectónicas. 2005. Trabajo de Grado. Universidad Nacional de Colombia. Medellín. 54 P.
- Zuluaga, C.A., Medina, P.A., and Martinez, L.F., 2008. A Cretaceous Subduction Zone in Northern Colombia (southern Caribbean plate)?.. Geological Society of America, Joint Annual Meeting, Abstract, pp. 128-6.

